Developmental Cell
Article

Pancreatic β Cell Identity Is Maintained by DNA Methylation-Mediated Repression of *Arx*

Sangeeta Dhawan,[1,4] Senta Georgia,[1,4] Shuen-ing Tschen,[1] Guoping Fan,[2] and Anil Bhushan[1,3,*]
[1]Department of Medicine
[2]Department of Human Genetics
[3]Molecular, Cell and Developmental Biology
University of California, Los Angeles, Los Angeles, CA 90095-7073, USA
[4]These authors contributed equally to this work
*Correspondence: abhushan@mednet.ucla.edu
DOI 10.1016/j.devcel.2011.03.012

SUMMARY

Adult pancreatic β cells can replicate during growth and after injury to maintain glucose homeostasis. Here, we report that β cells deficient in *Dnmt1*, an enzyme that propagates DNA methylation patterns during cell division, were converted to α cells. We identified the lineage determination gene aristaless-related homeobox (*Arx*), as methylated and repressed in β cells, and hypomethylated and expressed in α cells and *Dnmt1*-deficient β cells. We show that the methylated region of the *Arx* locus in β cells was bound by methyl-binding protein MeCP2, which recruited PRMT6, an enzyme that methylates histone H3R2 resulting in repression of *Arx*. This suggests that propagation of DNA methylation during cell division also ensures recruitment of enzymatic machinery capable of modifying and transmitting histone marks. Our results reveal that propagation of DNA methylation during cell division is essential for repression of α cell lineage determination genes to maintain pancreatic β cell identity.

INTRODUCTION

Terminally differentiated pancreatic β cells retain the capacity to proliferate during growth and after injury to maintain glucose homeostasis (Dor et al., 2004; Georgia and Bhushan, 2004; Teta et al., 2007; Zhong et al., 2007). This suggests that the gene expression pattern of β cells needs to be propagated with high fidelity to ensure that cell identity is maintained after cell division. The gene expression pattern of β cells is established during development, as the fates of pancreatic progenitor cells are progressively restricted. Genetic studies have identified a number of genes that are important for restricting cell fate choice within the different endocrine lineages. In particular, two homeobox genes, *Arx* and *Pax4*, are exclusively expressed in α and β cell lineages, respectively. Mice lacking *Arx* display increased numbers of β and δ cells at the expense of α cells (Collombat et al., 2003). Conversely, mice lacking *Pax4* display reduced β cells and increased in α cell numbers (Sosa-Pineda et al., 1997). Gain-of-function experiments show that forced misexpression of *Pax4* or *Arx* in α and β cells, respectively, can lead to cell fate conversion (Collombat et al., 2007, 2009). Furthermore, loss of another homeobox gene, *Nkx2.2*, results in increased epsilon cell mass at the expense of β cells (Prado et al., 2004). These studies suggest that repression of lineage determination genes plays a prominent role in establishing cell fate during development. However, the mechanisms responsible for the stable propagation of the repressed state of these key lineage determination genes during cell division are not well understood.

It is generally believed that the assembly of a specific chromatin structure that can be propagated through DNA replication and cell division accompanies heritable gene repression. How lineage-specific transcription factor networks interact with different epigenetic marking systems to achieve stability of cell identity is not clear. One mechanism that ensures stable inheritance of repressed genes involves covalent modification of DNA by methyl groups. DNA methylation patterns are faithfully reproduced during cell division by DNA methyltransferase, Dnmt1, which recognizes hemimethylated DNA to restore the symmetrical CpG methylation pattern (reviewed in Goll and Bestor, 2005; Klose and Bird, 2006; Miranda and Jones, 2007). However, the precise function of CpG methylation in gene repression has not been firmly established.

Here, we report that pancreatic β cells deficient in *Dnmt1* were reprogrammed to α cells. Using genome-wide analysis, we identified Arx to be methylated and repressed in β cells but hypomethylated and expressed in *Dnmt1*-deficient β cells. Methyl-specific binding proteins that recruit enzymatic machinery capable of locally altering histone modification bound the methylated region of *Arx* locus. Our results suggest that propagation of DNA methylation pattern forms the backbone for transmitting histone modifications and the assembly of *Arx*-repressive chromatin structure that can be stably inherited through cell division to preserve β cell identity.

RESULTS

Deletion of *Dnmt1* Converts β Cells into α Cells

To investigate the requirement for maintaining DNA methylation patterns during pancreatic β cell replication, we crossed mice transgenic for Cre recombinase under the control of rat insulin promoter (RIP-cre) with DNA methyltransferase (*Dnmt1*)$^{fl/fl}$

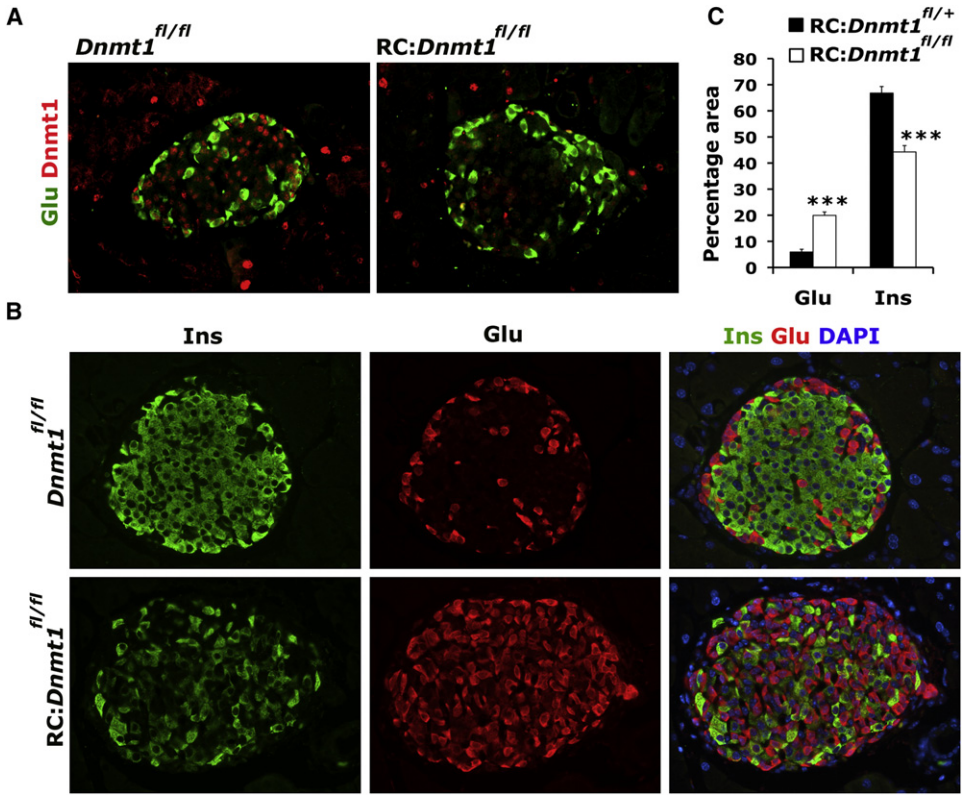

Figure 1. Loss of DNA Methylation in β Cells Results in an Increase in the Number of Glucagon-Expressing Cells

(A) Representative pancreatic sections from 3-month-old *Dnmt1*$^{fl/fl}$ (control) and RIP-Cre:*Dnmt1*$^{fl/fl}$ (RC:*Dnmt1*$^{fl/fl}$) littermates were immunostained for glucagon (Glu; green) and Dnmt1 (red).

(B) Immunostaining of representative pancreatic sections from 8-month-old *Dnmt1*$^{fl/fl}$ and RC:*Dnmt1*$^{fl/fl}$ littermates showing insulin (green), glucagon (red), and overlay with DAPI (to counterstain the nuclei; blue).

(C) Quantification of glucagon and insulin area in 8-month-old RIP-Cre:*Dnmt1*$^{fl/+}$ (control) and RIP-Cre:*Dnmt1*$^{fl/fl}$ animals, shown as percentage of total islet area (n = 4 animals). The error bars represent SEM (***p < 0.005).

See also Figure S1.

mice (Herrera, 2000; Jackson-Grusby et al., 2001) to selectively inactivate *Dnmt1* in β cells. Immunohistology confirmed cre recombinase activity specifically in β cells (see Figure S1A available online) and the absence of detectable Dnmt1 protein within the islets from pancreatic sections from RIP-Cre:*Dnmt1*$^{fl/fl}$ mice (denoted RC:*Dnmt1*$^{fl/fl}$, conditional *Dnmt1* mutant), whereas abundant Dnmt1 protein was observed within the islets of pancreatic tissue from *Dnmt1*$^{fl/fl}$ littermates (Figures 1A and S1B). Staining of pancreatic sections from conditional *Dnmt1* mutant mice with 5-methylcytosine antibody at different ages showed that islets from 3-month-old pancreas had relative uniform staining of 5-methylcytosine; however, islets from 8-month-old pancreas displayed patchy 5-methylcytosine staining (Figure S1C). Quantification of DNA methylation confirmed decrease in global DNA methylation in 8-month-old islets isolated compared to isolated islets from 6-week-old conditional *Dnmt1* mutant mice, whereas no changes in global DNA methylation were observed in isolated islets from similarly aged control mice (Figure S1D). β Cells have been shown to replicate in a homogenous fashion, and as the animal ages, a greater proportion of β cells within the islet would derive from replicating β cells. Thus, the absence of *Dnmt1* resulted in a passive loss of DNA methylation that correlated with the rate of β cell replication (Brennand et al., 2007; Teta et al., 2007). This led to a gradual increase in the number of β cells that lost cytosine methylation because greater numbers of β cell divide as the animal aged.

Pancreatic tissue isolated from mice at different ages was immunostained for insulin and glucagon, endocrine hormones that mark β and α cells, respectively. Islets from wild-type and conditional *Dnmt1* mutant littermates at birth did not show any differences and displayed a characteristic distribution of endocrine cells, with β cells forming the core and α cells at the periphery forming the mantle. Even though *Dnmt1* is deleted in β cells in young conditional *Dnmt1* mutant mice (Figure S1B), DNA methylation is not significantly different in these β cells (Figures S1C and S1D), consistent with the absence of an overt phenotype observed in the young conditional *Dnmt1* mutant mice. However, with increasing age (and increased β cell duplications along with passive demethylation), significant differences became apparent in conditional *Dnmt1* mutants, which displayed reduced DNA methylation, increased number of glucagon-expressing cells throughout the islet, whereas the number of insulin-expressing cells were diminished (Figure 1B; Figures S1C–S1E). Quantification of insulin and glucagon area

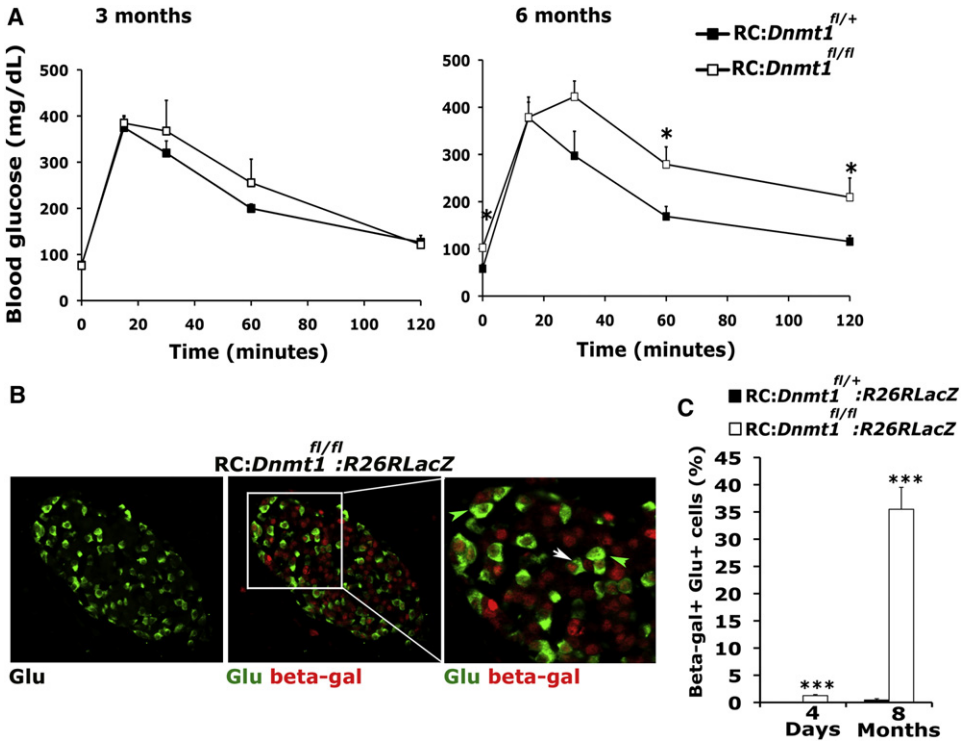

Figure 2. DNA Methylation Is Required for Maintenance of β Cell Identity

(A) Glucose tolerance test (GTT) for RC:*Dnmt1*$^{fl/+}$ (control) and RC:*Dnmt1*$^{fl/fl}$ animals at ages 3 months (left panel) and 6 months (right panel) (n = 5 for each genotype).

(B) Representative pancreatic section from an 8-month-old RC:*Dnmt1*$^{fl/fl}$:*R26RLacZ* animal showing immunostaining for glucagon (green) in the left panel and an overlay of glucagon with β-galactosidase (β-gal; red) in the middle panel. The inset marks a representative area, magnified and shown in right panel. A number of β-galactosidase and glucagon double-labeled cells (white arrows) are evident in these RC:*Dnmt1*$^{fl/fl}$:*R26RLacZ* animals. Green arrows indicate normal α cells, which express glucagon and do not stain for β-galactosidase.

(C) Quantification of endocrine cells costaining for glucagon and RIP-Cre driven β-galactosidase in RC:*Dnmt1*$^{fl/+}$:*R26RLacZ* (control) and RC:*Dnmt1*$^{fl/fl}$:*R26RLacZ* animals at 4 days and 8 months of age (n = 3 animals per group). The error bars represent SEM (***p < 0.005).

See also Figure S2.

in islets confirmed the increase in glucagon-expressing cells in conditional *Dnmt1* mutants (Figure 1C). Glucose tolerance tests showed that with increasing age the conditional *Dnmt1* mutants mice displayed abnormal glucose homeostasis, consistent with the reduction in β cells (Figure 2A). To assess whether these excessive glucagon-expressing cells originated from β cells, cells transcribing the insulin gene were heritably labeled using the R26R-*LacZ*, or R26R-*YFP* reporters to reveal that a number of glucagon-expressing cells observed in the conditional *Dnmt1* mutant pancreas indeed derived from cells that had transcribed the insulin gene (Figure 2B; Figures S2A and S2B). The number of glucagon-expressing cells that also displayed enzymatic β-galactosidase activity increased dramatically in older conditional *Dnmt1* mutants (Figure 2C).

Dnmt1 Propagates DNA Methylation of α Cell Lineage Determinant *Arx*

We hypothesized that key determinants of the α cell lineage were methylated and repressed to maintain β cell lineage stability, and these determinants were derepressed in the β cells deficient in DNA methylation. To identify such methylated α cell lineage determinants, we carried out genome-wide mapping of DNA methylation patterns at 5′ upstream promoter regions using the methylated DNA immunoprecipitation (MeDIP) method (Weber et al., 2005). Methylated CpG-enriched DNA fractions using anti-5-methyl cytosine antibody were collected from mouse α and β cell lines (α-TC1 and Min6) and hybridized to high-resolution promoter microarrays. We screened for 5′ upstream regulatory regions that showed higher methylation levels in Min6 cells when compared with α-TC1 cells. Analysis of the methylation profiles of endocrine cell fate determination genes led to the identification of two CpG-rich regions in the 5′ regulatory region of *Arx* that were differentially methylated in Min6 and α-TC1 cells (Figure S3A). Overexpression of *Arx* in Min6 cells was sufficient to repress β cell markers and induce α cell markers, suggesting that Arx plays a crucial role in α cell fate (Figures S3B and S3C). This is consistent with previous studies showing that *Arx* is not expressed in the β cells, and misexpression of *Arx* in β cells can respecify them to an α cell fate (Collombat et al., 2003, 2005, 2007). This suggested that methylation of *Arx* regulatory regions in β cells may correlate to its repression in β cells.

The *Arx* regulatory region is characterized by several CpG-rich sites. We focused on two of these: one within the proximal promoter and close to the transcription start site (TSS), referred

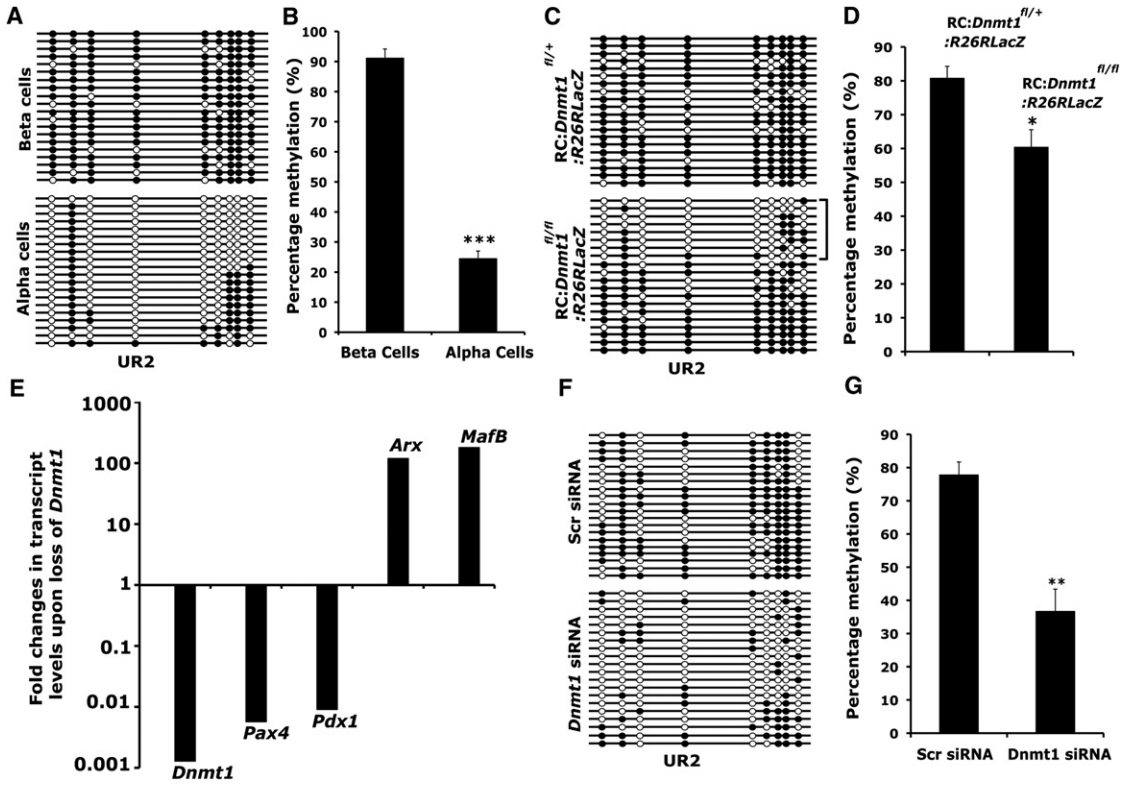

Figure 3. *Dnmt1* Methylates and Leads to the Repression of *Arx* Locus in β Cells

(A) Bisulfite-sequencing analysis and (B) quantification of the bisulfite-sequencing data, shown as percent DNA methylation (n = 3) for the CpG-rich UR2 region of *Arx* locus (−2103 to −1992 bp) in isolated β and α cells.

(C) Bisulfite-sequencing analysis and (D) quantification of the bisulfite-sequencing data, shown as percent DNA methylation (n = 3), for the UR2 region of *Arx* locus in cells marked with β-galactosidase activity from RIP-Cre:*Dnmt1*$^{fl/fl}$:*R26RLacZ* (RC:*Dnmt1*$^{fl/fl}$:*R26RLacZ*) animals. Littermate RC:*Dnmt1*$^{fl/+}$:*R26RLacZ* mice were used as controls. Each horizontal line with dots is an independent clone, and 20 clones are shown here. The UR2 region is almost fully DNA methylated (filled circles) in β cells but largely hypomethylated (open circles) in α cells. Cells isolated using β-galactosidase activity from RC:*Dnmt1*$^{fl/fl}$:*R26RLacZ* animals showed a subset of clones that were hypomethylated, as marked by the bracket (*$p < 0.05$).

(E) Fold changes in the levels of *Dnmt1*, *Pax4*, *Pdx1*, *MafB*, and *Arx* transcripts determined by real-time RT-PCR in the cells marked with β-galactosidase activity from RC:*Dnmt1*$^{fl/fl}$:*R26RLacZ* and control littermates, with the levels in control set as one arbitrary unit. The levels are depicted on a logarithmic scale.

(F) Bisulfite-sequencing analysis and (G) quantification of the bisulfite-sequencing data, shown as percent DNA methylation (n = 3), for the UR2 region of *Arx* promoter from Min6 cells treated with control, scrambled (Scr), or *Dnmt1* siRNAs. The error bars represent SEM (**$p < 0.01$).

See also Figure S3.

to as UR1, and another one 2 kb upstream of TSS, termed UR2. Detailed characterization of the *Arx* upstream regulatory region methylation profiles by bisulfite-sequencing analysis in FACS-purified α and β cells revealed that a vast majority of CpG dinucleotides in UR2 region were methylated in β cells but unmethylated in α cells, whereas no difference in DNA methylation was observed in UR1 region (Figure 3A; Figure S3D). Quantification of DNA methylation of the UR2 region revealed significantly reduced DNA methylation in isolated DNA from sorted α cells compared to sorted β cells (Figure 3B). A region 2.5 kb upstream of TSS, named UR3, was also identified in the MeDIP screens along with UR2 and showed differential methylation patterns similar to the UR2 region (Figures S3E and S3F). However, no significant differences in DNA methylation were observed in the 3′ conserved enhancer region identified in previous studies (Figure S3G), suggesting that regulation of *Arx* expression by this downstream enhancer region is not dependent on DNA methylation (Collombat et al., 2005). Furthermore, bisulfite analysis of a CpG-rich region +1292 to +1400 bp region within intron 1 showed no significant differences in α and β cells (Figure S3H).

To investigate whether β cells deficient in *Dnmt1* displayed changes in DNA methylation at these CpG-rich regions of the *Arx* locus, we used the R26R-*LacZ* reporter to isolate heritably labeled cells that transcribed the insulin gene, using β-galactosidase activity to cleave a fluorescent substrate, followed by FACS. Bisulfite-sequencing analysis on β-galactosidase positive cells isolated from control mice showed a heavily methylated pattern in the UR2 region similar to the pattern observed in purified β cells. In contrast, β-galactosidase positive cells isolated from conditional *Dnmt1* mutant littermates revealed two distinct patterns of methylation on the UR2 region of the *Arx* gene, indicating clonal heterogeneity. One set of clones was methylated, characteristic of β cells, whereas the other set of clones was predominately unmethylated and characteristic of α cells (Figure 3C). The heterogeneity is consistent with the fact that isolated cells from *Dnmt1*-deficient mice would be a mixed

population consisting not only of undivided β cells that retained genomic patterns of cytosine methylation but also the progeny of divided cells that lost cytosine methylation. These results indicate that *Arx* gene was unmethylated in the progeny of divided β cells of conditional *Dnmt1* mutant mice (Figure 3D). In addition, isolated β cells from conditional *Dnmt1* mutant mice showed massive increase in the expression of *Arx* compared to β cells isolated from wild-type littermates, along with another α cell marker *MafB* and significant reduction in the levels of β cell markers *Pdx1* and *Pax4* (Figure 3E). To determine whether DNA methylation directly correlated with *Arx* repression, we performed knockdown of *Dnmt1* in Min6 cells using specific small inhibitory RNA (siRNA). Bisulfite-sequencing analysis of *Dnmt1*-deficient Min6 cells showed that loss of *Dnmt1* resulted in loss of methylation at the UR2 region of *Arx*, resulting in a methylation profile similar to purified α cells (Figures 3F and 3G). Furthermore, *Dnmt1*-deficient Min6 cells displayed increase in the expression of *Arx* (Figure S3I). These experiments indicate that repression of *Arx* in β cells correlates with methylation of the *Arx* promoter. In the absence of *Dnmt1*, the loss of *Arx* promoter methylation results in derepression of the *Arx* locus.

Recruitment of PRMT6 at Methylated Region of *Arx* Facilitates Repression

We next sought to establish the mechanism by which DNA methylation facilitated the transcriptional repression of the *Arx* locus, by screening for methyl-DNA binding (MDB) proteins that bound the UR2 region of the *Arx* locus in β cells. Chromatin immunoprecipitation (ChIP) analysis showed that one member of the methyl-binding protein family (Bird, 2002), MeCP2, was bound to the UR2 region of the *Arx* promoter in β cells, but not in α cells (Figure 4A). Binding of MeCP2 to the UR2 regions of *Arx* locus was also significantly reduced in sorted β-galactosidase positive cells isolated from conditional *Dnmt1* mutant mice (Figure S4A). In addition to the MDB domain, MeCP2 has a transcriptional repressive domain that recruits enzymatic machinery capable of altering histone modification and regulating chromatin structure (Jones et al., 1998; Nan et al., 1998). To identify the binding partners of MeCP2, we transfected a Flag-tagged MeCP2 into Min6 cells and used an anti-Flag antibody to precipitate MeCP2-associated proteins. This analysis revealed several specific bands that coimmunoprecipitated with MeCP2, including one around 42 kDa (Figure S4B). Mass spectrometry analysis of this band identified PRMT6 (protein arginine methyltransferase 6) to be one of the proteins interacting with MeCP2, among others. PRMT6 resides predominantly in the nucleus and acts as a H3R2 methyltransferase and represses transcription by counteracting H3K4 trimethylation (Hyllus et al., 2007). To confirm the specificity of the above interaction, immunoprecipitates of Flag-tagged MeCP2-transfected Min6 cells subjected to western blotting using the PRMT6 antibody revealed that PRMT6 coprecipitated with MeCP2 (Figure 4B). These data were verified by immunoprecipitations using a myc-tagged PRMT6 overexpression construct to complex with MeCP2 (Figure 4C).

To further analyze whether PRMT6 bound to the methylated UR2 region of the *Arx* promoter, we measured the binding of PRMT6 by ChIP assays. ChIP analysis showed that PRMT6 was bound to the *Arx* locus in β cells where the UR2 region is methylated, whereas no binding of PRMT6 to the *Arx* locus was observed in α cells where the UR2 region is unmethylated (Figure 4D). The UR3 region, which is differentially methylated in β cells as well, is also specifically bound by MeCP2 and PRMT6 (Figure S4C), whereas the downstream regions that were not differentially methylated were not bound by these proteins (Figure S4D). Taken together, these data indicate that a complex containing MeCP2 and PRMT6 is recruited to the methylated regions of the *Arx* promoter and could play a role in the assembly and propagation of repressive chromatin structure of *Arx* locus.

We then assessed whether recruitment of PRMT6 to the methylated UR2 region of the *Arx* locus could play a role in the assembly and propagation of the repressive chromatin state of the *Arx* locus. We first measured levels of asymmetric dimethylation of H3R2 (H3R2me2a) at the *Arx* promoter in FACS-purified β and α cells. ChIP analysis using anti-H3R2me2a antibody showed high levels of enrichment at the *Arx* promoter in β cells and low binding in α cells (Figure 4E). As recent studies have shown that H3K4 methylation is antagonized by PRMT6-mediated H3R2me2a (Guccione et al., 2007; Hyllus et al., 2007; Kirmizis et al., 2007), we sought to determine the methylation levels of H3K4 by ChIP analysis using an anti-H3K4me3 antibody. These experiments revealed high levels of H3K4me3 at the *Arx* locus in α cells, whereas H3K4 was unmethylated at the *Arx* promoter in β cells (Figure 4E). Sorted β-galactosidase positive cells isolated from conditional *Dnmt1* mutant mice displayed high levels of H3K4me3 and low levels of H3R2me2a similar to sorted α cells (Figure S4E). Analysis of the levels of H3K9 dimethylation and trimethylation (H3K9me2 and H3K9me3) at the *Arx* locus by ChIP showed high levels of these two histone modifications in β cells, confirming a repressed chromatin state of *Arx* locus (Figure 4E). ChIP analysis using anti-H3K9/14ac and HDAC1 antibodies showed very low levels of histone acetylation at the *Arx* locus (Figure 4E), which correlated with recruitment of HDAC1 to the *Arx* locus in β cells compared to α cells (Figure S4F).

DNA Methylation Propagates the Transcriptional Repression of *Arx* during β Cell Replication

To test whether DNA methylation is involved in maintaining *Arx* chromatin structure for many generations of actively dividing cells, we treated Min6 cells with *Dnmt1* siRNA to assess cell numbers, DNA methylation, and histone modifications on *Arx* locus. Bisulfite-sequencing analyses showed progressive loss of methylation within the UR2 region of the *Arx* locus with increase in cell duplications (Figure 5A; Figure S5A). ChIP analysis revealed that decreased methylation within the UR2 region of *Arx* locus upon loss of *Dnmt1* correlated with reduced binding of MeCP2 (Figure 5B). We also observed a reduction in H3R2me2a levels and an increase in H3K4me3 levels, suggesting that histone modifications profile of the *Arx* locus was altered (Figure 5C). Furthermore, reduced levels of H3K9me2 and H3K9me3 and increased levels of H3K9Ac confirmed the open chromatin structure of *Arx* locus in the absence of *Dnmt1* (Figure S5B). These results suggest that loss of DNA methylation over several cell divisions can lead to derepression of the *Arx* locus. We then asked whether changes in *Arx* chromatin structure that resulted in derepression of the *Arx* locus led to changes in gene expression profile of the cell. Expression analysis of

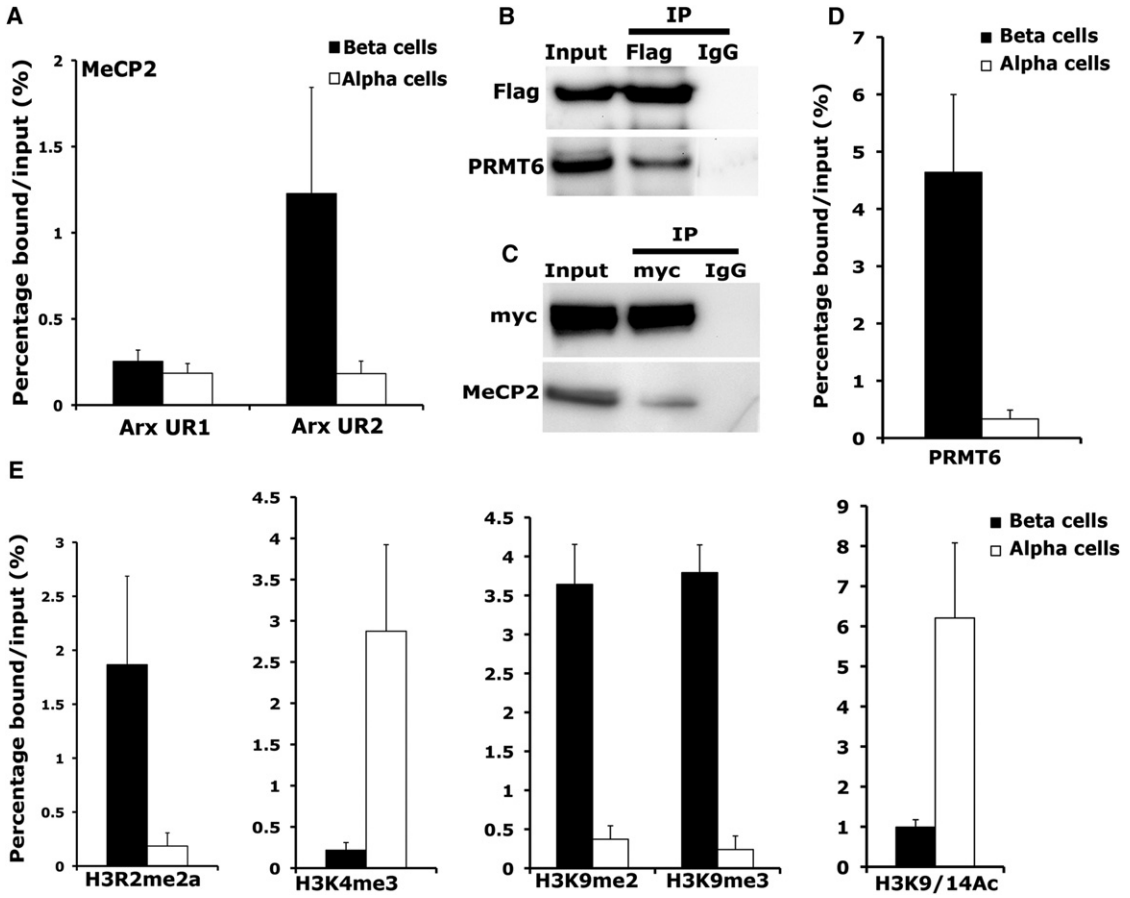

Figure 4. MeCP2 Binds to the *Arx* Locus in β Cells and Recruits H3R2 Methyltransferase PRMT6 to Repress *Arx* Expression

(A) ChIP analysis showing the binding of MeCP2 to the two CpG-rich regions, UR2 (−2111 to −1960 bp) and UR1 (−184 to −254 bp), of the *Arx* locus in β and α cells.

(B) Coimmunoprecipitation analysis examining the interaction of MeCP2 and PRMT6. Cell extracts from Min6 cells transfected with Flag-MeCP2 construct were used as INP for immunoprecipitation (IP) with anti-Flag antibody and analyzed by immunoblotting with Flag and PRMT6 antibodies.

(C) Coimmunoprecipitation analysis for the interaction of PRMT6 with MeCP2 using IP with myc-tag antibody on Min6 cells transfected with myc-PRMT6 construct, and western blotting with myc-tag and MeCP2 antibodies.

(D) ChIP analysis comparing the recruitment of PRMT6 to the UR2 region of *Arx* locus in β and α cells.

(E) ChIP analysis comparing the levels of asymmetric H3R2 dimethylation (H3R2me2a), H3K4 trimethylation (H3K4me3), H3K9 dimethylation and trimethylation (H3K9me2 and H3K9me3), and H3K9/14 acetylation (H3K9/14Ac) at the differentially methylated UR2 region of the *Arx* locus in β and α cells purified from 5-month-old wild-type mice. These analyses indicate enrichment of histone modification associated with repression of gene expression, namely H3R2me2a, H3K9me2, and H3K9me3 at the *Arx* locus in pancreatic β cells. The error bars represent SEM.

See also Figure S4.

a number of endocrine markers by quantitative PCR analysis revealed that *Dnmt1* siRNA-treated Min6 cells after several cell divisions had reduced levels of β cells markers *Pdx1*, *Pax4*, and *Insulin* (*Ins*). In contrast, the expression of α cell markers, *Arx*, *Mafb*, and *Glucagon* (*Glu*), was increased, suggesting that Min6 cells no longer retained resemblance to β cells but instead expressed markers characteristic of α cells (Figure 5D). However, a combined knockdown of *Dnmt1* and *Arx* in Min6 cells did not result in any reduction in β cell markers or lead to induction of glucagon expression, indicating that derepression of *Arx* is critical to the cell fate switch upon loss of *Dnmt1* in β cells (Figure 5E).

Our analysis suggested that a complex containing MeCP2 and PRMT6 was recruited to the methylated regions of *Arx* locus to repress its expression in β cells. To test whether loss of MeCP2 or PRMT6 would mimic loss of Dnmt1, we performed loss-of-function studies for *MeCP2* and *Prmt6* in Min6 cells using specific siRNAs. Loss of *MeCP2* in Min6 cells resulted in derepression of the *Arx* locus, with concomitant upregulation of other α cell markers *Glu* and *MafB*, and a reduction in the levels of β cell markers, such as *Pdx1*, *Pax4*, and *Ins* (Figure 6A). These changes corresponded with reduced binding of MeCP2 and PRMT6 to the *Arx* locus, which also reflected in reduced levels of H3R2me2a and increased levels of H3K4me3 (Figures 6B and 6C). Similarly, loss of *Prmt6* resulted in expression of *Arx* in Min6 cells, accompanied by induction of other α cell markers and loss of β cell markers (Figure 6D). This was accompanied by loss of PRMT6 and MeCP2 binding to the *Arx* locus, leading to reduced H3R2me2a and increased H3K4me3 enrichment (Figures 6E and 6F). Thus, loss of *MeCP2* and *Prmt6* in Min6 cells

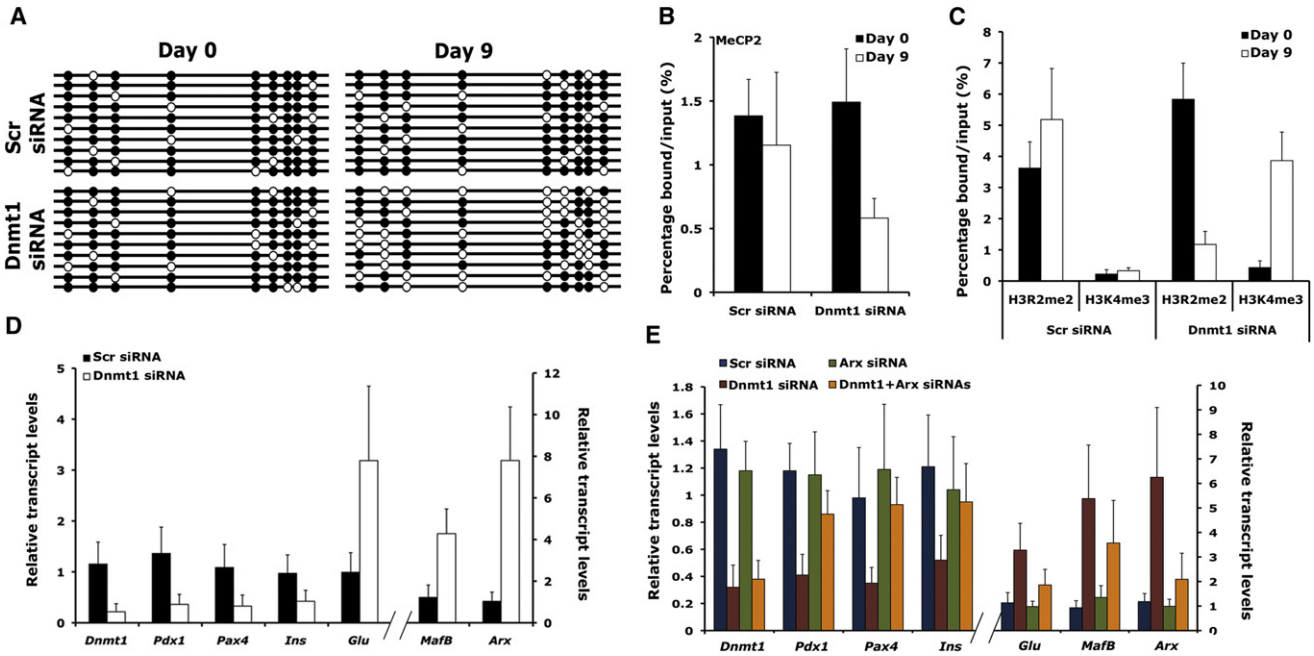

Figure 5. Loss of DNA Methylation Affects the Inheritance of the Repressive Histone Modifications on the *Arx* Locus in Successive Cell Generations

Min6 cells transfected with scrambled or *Dnmt1* siRNAs were grown in the exponential phase for 9 days in culture before cells were harvested.

(A) Bisulfite sequencing of the UR2 region of Arx locus in Min6 cells transfected with *Dnmt1* siRNA, harvested at days 0 and 9. The UR2 region of the *Arx* locus that is almost fully DNA methylated (filled circles) at the start of the experiment and is hypomethylated (open circles) after 9 days of exponential growth.

(B and C) ChIP analyses in Min6 cells transfected with scrambled or *Dnmt1* siRNAs, 0 and 9 days after transfection. The binding of MeCP2 to the UR2 region of *Arx* locus was reduced in *Dnmt1* siRNAs transfected Min6 cells at day 9 (B). At day 9 the levels of H3R2me2a were reduced, and H3K4me3 was increased in *Dnmt1* siRNA-transfected Min6 cells (C).

(D) Real-time RT-PCR analyses comparing the transcript levels of *Dnmt1*, *Pdx1*, *Pax4*, *Ins*, *Glu*, *MafB*, and *Arx* in Min6 cells after 0 and 9 days of transfection with *Dnmt1* or control, scrambled (Scr) siRNAs.

(E) Transcript levels of *Dnmt1*, *Pdx1*, *Pax4*, *Ins*, *Glu*, *MafB*, and *Arx* determined by real-time RT-PCRs in Min6 cells, after 9 days of transfection with scrambled (Scr), *Dnmt1*, *Arx*, or *Dnmt1+Arx* siRNAs, showing a requirement for *Arx* in cell fate conversion upon loss of *Dnmt1* (n = 3 for each experiment). The error bars represent SEM.

See also Figure S5.

was able to phenocopy the loss of *Dnmt1*, highlighting the functional importance of DNA methylation in regulation of *Arx*. This requirement for DNA methylation was further confirmed by treating Min6 cells with 5-aza-dC, a chemical that leads to DNA demethylation. Loss of DNA methylation due to 5-aza-dC treatment also resulted in loss of MeCP2 and PRMT6 binding at the *Arx* locus, concomitant with the induction of *Arx* expression, along with other α cell markers *Glu* and *MafB*, and reduction in the expression of β cell markers, such as *Pdx1*, *Pax4*, and *Ins* (Figures S6A–S6D). This suggests that DNA methylation can influence the covalent histone modification patterns to perpetuate a repressed chromatin state of the *Arx* locus and maintain β cell identity. Taken together, these results indicate that DNA methylation plays an active role in the assembly of chromatin structure to repress transcription of α cell determination gene *Arx* to maintain β cell identity.

DISCUSSION

It has been generally assumed that the identity of adult differentiated cells is fixed, although there is emerging evidence that adult cells can be manipulated to change identity (Takahashi and Yamanaka, 2006; Vierbuchen et al., 2010; Zhou et al., 2008) or regain plasticity (Collombat et al., 2009; Thorel et al., 2010). Understanding the mechanisms that preserve cell identity would enable successful manipulation of cell plasticity in clinical settings. Our work reveals that *Arx*, a key determination gene for α cells, is methylated and repressed in pancreatic β cells. Dnmt1 propagates this methylation during cell division to ensure repression of *Arx* in the progeny and preservation of β cell identity. Deletion of *Dnmt1* in β cells results in the derepression of *Arx* and a gradual conversion to α cell-like identity. There are several reasons why the switch in cell identity occurs gradually. First, Dnmt1 primarily maintains methylation patterns during cell division, and the effects of *Dnmt1* deletion are only apparent in the progeny of cells that lack *Dnmt1*. Deletion of *Dnmt1* leads to passive demethylation that is linked to the rates of β cell replication. BrdU-labeling studies demonstrate that all β cells are uniformly capable of cell division, and newly divided β cells are prevented from reentering the cell cycle after cell division (Brennand et al., 2007; Teta et al., 2007). Second, β cell replication declines with age, resulting in fewer β cells undergoing successive rounds of cell division (Dhawan et al., 2009; Rankin and Kushner, 2009; Tschen et al., 2009).Third, cells displaying

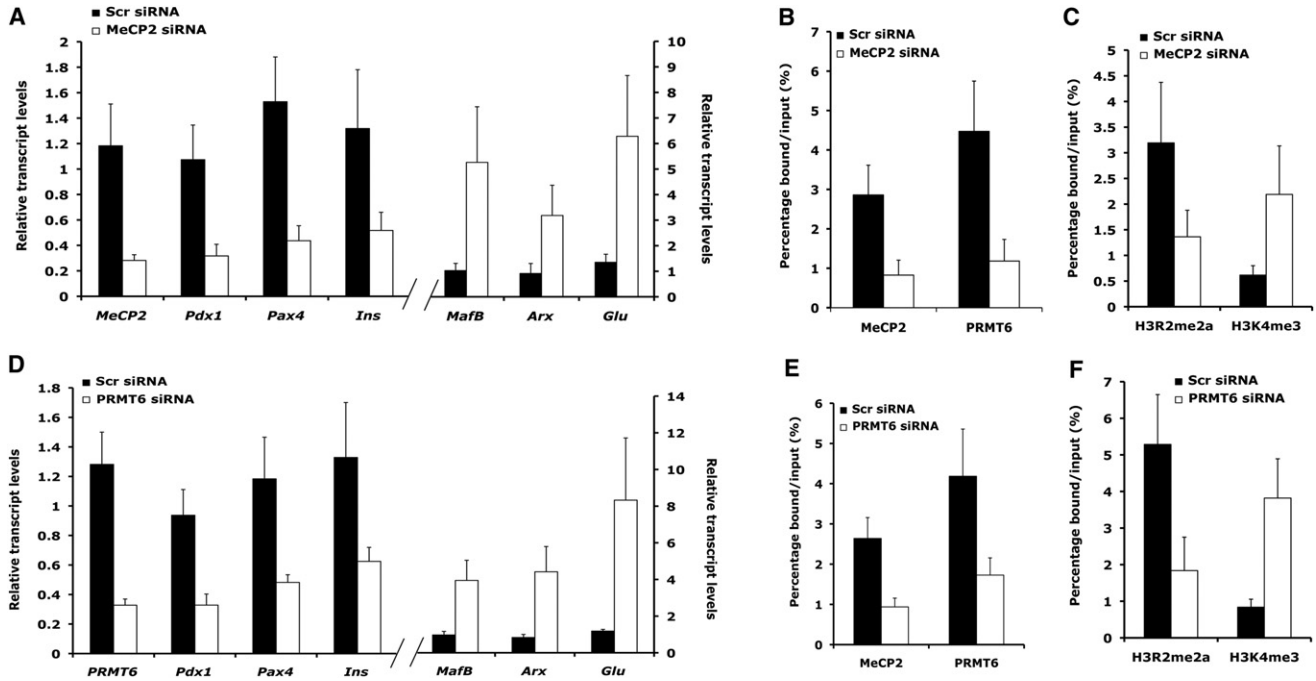

Figure 6. Inhibition of MeCP2 and PRMT6 Phenocopies the Loss of Dnmt1

(A) Transcript levels of *MeCP2*, *Pdx1*, *Pax4*, *Ins*, *Glu*, *MafB*, and *Arx* determined by real-time RT-PCRs, (B) binding of MeCP2 and PRMT6 to the UR2 region of *Arx* locus, and (C) levels of H3R2me2a and H3K4me3 at the UR2 region of the *Arx* locus in Min6 cells, after 9 days of transfection with scrambled (Scr) and *MeCP2* siRNAs.

(D) Transcript levels of *Prmt6*, *Pdx1*, *Pax4*, *Ins*, *Glu*, *MafB*, and *Arx* determined by real-time RT-PCRs, (E) binding of MeCP2 and PRMT6 to the UR2 region of *Arx* locus, and (F) levels of H3R2me2a and H3K4me3 at the UR2 region of the *Arx* locus in Min6 cells, after 9 days of transfection with scrambled (Scr) and *Prmt6* siRNAs.

See also Figure S6.

costaining of insulin and glucagon are observed in mice with *Dnmt1* deletion in β cells and could correspond to cells displaying intermediate stages in the cell identity switch. This implies that the switch in between β and α cell-like identity is not immediate but gradual and is reminiscent of somatic cell reprogramming during which cells in different stages of reprogramming are observed (Hanna et al., 2009). All of these factors can contribute to the slow kinetics of cell conversion observed in mice that lack *Dnmt1* in β cells.

It is noteworthy that loss of *Dnmt1* in pancreatic β cells did not lead to large-scale derepression of silent tissue-specific genes. Our results suggests that DNA methylation regulated repression of a small set of genes involved in lineage specification of cell types that are closely related in developmental history. It is likely that a larger set of genes is regulated by DNA methylation, but only genes that have appropriate transcriptional activator present will be derepressed in *Dnmt1*-deleted cells. Studies in ES cells also show that DNA methylation regulation of a single transcription factor plays a role in the separation of embryonic and trophoblast lineages. *Elf5* is hypomethylated and expressed in trophoblast cells, but DNA methylation stably represses *Elf5* in the embryonic lineage. Deletion of *Dnmt1* allows for efficient differentiation of methylation-deficient ES cells into the trophoblast lineage (Ng et al., 2008). Other studies also suggest that methylation of a lineage determination gene regulates astrocyte differentiation in the developing brain and T cell development, suggesting that regulation of a limited number of genes is likely to be a general feature of DNA methylation-dependent gene repression (Lee et al., 2001; Takizawa et al., 2001).

Our study highlights the crucial role of DNA methylation in the epigenetic inheritance of a cell differentiation state. Our work here provides a molecular link by which gene repression by DNA methylation is accompanied by the alterations in histone modifications and the assembly of a specific chromatin structure that can be stably inherited through cell division to preserve cell identity. Several studies suggest that methylated CpG-binding proteins recruit enzymatic machinery capable of locally altering histone modifications that can maintain chromatin structure through many cell cycles. Histone modifiers such as HDACs and Sin3A associate with MeCP2, potentially linking DNA methylation-dependent silencing with changes in chromatin modifications (Jones et al., 1998; Nan et al., 1998). In this study, we have identified PRMT6, an H3R2 methyltransferase, as a interaction partner of MeCP2, which results in CpG methylation-directed asymmetric dimethylation of H3R2, a histone modification associated with repression of transcription (Guccione et al., 2007; Hyllus et al., 2007). Our data establish a direct correlation between DNA methylation and establishment of a repressive chromatin structure dependent on DNA methylation. This supports a model in which propagation of methylation pattern DNA forms the backbone for transmitting histone modifications that regulate the assembly of repressive chromatin

structure to the next cell generation (Martin and Zhang, 2007). Finally our results show that inheritance of epigenetic information can regulate pancreatic endocrine cell identity, suggesting that epigenetic reprogramming of cell types with shared developmental history could be an effective strategy for pancreatic β cell-replacement therapies for diabetes. Taken together, this study can form a basis for how inheritance of epigenetic information during cell division can be exploited for cell replacement therapies.

EXPERIMENTAL PROCEDURES

Animals, Metabolic Testing, and Cell Lines

We used Cre/loxP system to conditionally delete *Dnmt1* in pancreatic β cells. *Dnmt1*$^{fl/fl}$ mice with loxP sites flanking exons 4 and 5 of the *Dnmt1* gene and RIP-Cre mice expressing Cre-recombinase from rat insulin promoter have been described previously (Herrera, 2000; Jackson-Grusby et al., 2001). The RIP-Cre mice were bred into the Rosa26R-*LacZ* or Rosa26R-*YFP* background to indelibly mark all cells that were derived from insulin-expressing cells (Jackson Labs) (Soriano, 1999). All animal experiments were performed in accordance with NIH policies on the use of laboratory animals and approved by the Animal Research Committee of the Office for the Protection of Research Subjects at UCLA. Glucose tolerance test was performed following overnight fasting of the animals, as previously described (Zhong et al., 2007). Min6 cells were maintained in DMEM containing 10%FBS and 25 mM glucose at 37°C in 5% CO_2 environment. α-TC1 cells were cultured in DMEM containing 16.8 mM glucose, 4 mM L-glutamine, 17.8 mM $NaHCO_3$, and 10% FBS at 37°C in 5% CO_2 environment.

Immunofluorescence Staining and Morphometric Analysis

Standard immunofluorescence protocol was used for immunodetection of various proteins in pancreatic sections (Zhong et al., 2007). Briefly, pancreatic tissue was dissected in PBS, fixed in 4% formaldehyde for 4 hr to overnight, dehydrated in grades of ethanol, and stored in −20°C until processed for paraffin embedding. Primary antibodies were diluted in the blocking solution at the following dilutions: Mouse anti-Glucagon (diluted 1:1000; Sigma-Aldrich G2654-.2ML); rabbit anti-Glucagon (diluted 1:500; ImmunoStar 20076); guinea pig anti-Insulin (diluted 1:400; Dako A0564); mouse anti-Dnmt1 (diluted 1:5000; Imgenex IMG-261A); chicken anti-β-galactosidase (1:1500; Abcam ab9361); mouse anti 5-methyl cytosine (1:200; Aviva Systems Biology AMM99021); and chicken anti-GFP (1:500; Aves Labs, Inc., 1020). Donkey- and goat-derived secondary antibodies conjugated to FITC or Cy3 were diluted 1:500 (Jackson ImmunoResearch Laboratories). Slides were viewed using a Leica DM6000 microscope, and images were acquired using Openlab software (Improvision). For measurement of insulin and glucagon-positive cell areas, 30 randomly chosen islets per animal (four animals per group) from pancreatic sections immunostained for insulin and glucagon expression were imaged as above. Islets were defined as individual regions of interest, and total area along with the area of insulin and glucagon staining was quantified. Measurements of insulin and glucagon staining are expressed as a percentage of individual islet area. For calculation of glucagon cells coexpressing RIP-Cre driven β-galactosidase lineage trace, total β-galactosidase positive cells were counted along with cells double positive for β-galactosidase and glucagon in 30 randomly chosen islets per animal (three animals per group), and the data were expressed as percentage of double-positive cells.

Islet Isolation and Cell Sorting

Islets were isolated using the Liberase enzyme blend (Roche Diagnostics) as described before (Zhong et al., 2007). For α cell isolation, islets from wild-type mice were digested into a single-cell suspension and immunostained for glucagon, following brief fixation with BD Cytofix reagent (BD PharMingen), using rabbit anti-glucagon antibody, followed by incubation with a Cy3-conjugated secondary antibody, and sorted by FACS to an average percent purity of 80%–85%. Islet cells processed without primary antibody were used as a negative control for FACS. For purification of β cells, islets from MIP-GFP transgenic mice were digested into single cells and sorted for GFP by FACS to an average percent purity of 85%–95%. Cells from wild-type islets were used as negative control for FACS gating. β cell-derived endocrine cell lineage traced with β-galactosidase activity driven by RIP-Cre was purified after cleavage of fluorescent substrate fluorescein di-b-D-galactopyranoside (FDG; Sigma-Aldrich), by FACS sorting. For FACS sorting of these β-galactosidase positive cells, single-cell suspension was prepared from isolated islets in ice-cold FACS buffer (1× HBSS with 2% serum) and divided into 100 μl aliquots. One hundred microliter aliquots of 2 mM FDG in amber tubes were prewarmed at 37°C for 10 min along with cell aliquots. The cells were transferred to tubes with FDG and incubated at 37°C for 1 min. The reaction was stopped by the addition of 2 ml ice-cold sorting buffer, followed by incubation on ice for 30 min and subsequently at room temperature for 1 hr. Cells were spun down, washed, suspended in sorting buffer, and sorted.

siRNA-Based Knockdown, RNA Isolation, cDNA Synthesis, Real-Time PCRs

Knockdown of *Dnmt1*, *Arx*, and *Dnmt1+Arx* in Min6 cells was performed by transfection with a pool of specific-targeting siRNAs (siRNA, purchased from Dharmacon Research Inc.), using Lipofectamine-2000 (Invitrogen) according to manufacturer's instructions using OPTI-MEM medium. Min6 cells were transfected with appropriate siRNAs or scrambled controls every 3 days (average transfection efficiency 65%–80%), and samples were harvested after transfection, as indicated. RNA was isolated from dissected pancreatic tissue or islets using TRI Reagent (MRC) and treated with DNase (Ambion) according to manufacturers' instructions. RNA from sorted cells was prepared using RNeasy Micro Kit (QIAGEN). One microgram of RNA was used for preparation of single-stranded cDNA using Superscript III Reverse Transcriptase (Invitrogen) by the oligodT priming method. Real-time RT-PCRs were performed using the LightCycler FastStartPLUS DNA SYBR Master kit (Roche) and the Light Cycler PCR equipment (Roche). The expression levels of each transcript were normalized to the housekeeping gene *Cyclophilin*. Each real-time PCR experiment shown is a representative from at least three independent experiments; for each experiment, islets were pooled from three to four mice per specified group. Real-time PCR primers for RT-PCR are listed in Supplemental Experimental Procedures.

Coimmunoprecipitation Analyses

A total of 2.5 μg of antibody (or control IgG) was immobilized onto Protein-A or Protein G Sepharose (Millipore, Bedford, MA, USA) and washed with cold nondenaturing buffer (20 mM Tris-HCl [pH 8], 137 mM NaCl, 10% glycerol, 1% NP-0, 2 mM EDTA). The antibody-coated beads were bound with cellular extracts prepared from Min6 cells (either untransfected or transfected with the appropriate expression construct) in the nondenaturing buffer and incubated 5–16 hr at 4°C with shaking. Beads were washed three times in ice-cold nondenaturing buffer and eluted into SDS-PAGE gel loading buffer. The immunoprecipitates were analyzed by western blotting with appropriate antibodies. Western blots with the indicated antibodies were performed as described before (Zhong et al., 2007). Liquid chromatography-mass spectrometry analysis was used to identify proteins coimmunoprecipitating with MeCP2, in Min6 cells, as described in Supplemental Experimental Procedures.

DNA Methylation Analyses and ChIP Analyses

Bisulfite conversion of DNA was performed as described previously (Millar et al., 2002). DNA samples were incubated with sodium bisulfite for 4–5 hr. Bisulfite-treated DNA was then desalted and precipitated. One-tenth of precipitated DNA was used for each PCR using primers described in Supplemental Experimental Procedures to generate PCR products. Primers were designed using the MethPrimer software (Urogene). PCR products were gel purified and used for TOPO-TA cloning (Invitrogen), followed by sequencing. Primers used for generating bisulfite PCR products are described in Supplemental Experimental Procedures, under "Experimental Procedures" section. MeDIP was performed according to standard methods (Weber et al., 2005). For MeDIP, 4 μg of sonicated genomic DNA (size: 300–1000 bp) was immunoprecipitated (IP) with 5 μg of antibody against 5-methyl cytidine (5 mC; Aviva Systems Biology AMM99021) and collected for 4 hr at 4°C with constant agitation using Protein G magnetic beads (Dynabeads; Invitrogen). A portion of the sonicated DNA was kept aside as input (INP) control. DNA

was recovered from INP and IP by Proteinase-K$^+$ digestion, followed by phenol extraction and ethanol precipitation. Two hundred nanograms of IP and INP DNA were prepared for hybridization on the as per manufacturer's instruction for Mammalian ChIP-on-chip hybridization to the mouse whole genome promoter array (Agilent). The arrays were scanned using the Agilent DNA microarray scanner. Data extraction and analyses were performed using the Agilent Feature Extraction software (version 9.1.3.1). Probe signals were normalized with Lowess normalization and then extracted in 16 stepwise 500 bp windows covering −5.5 to +2.5 kb promoter regions, with reference to the TSS for each gene (Xie et al., 2009). ChIP experiments with the purified α and β cells were carried out using the micro-ChIP protocol (Dahl and Collas, 2008). The primers used to amplify the *Arx* locus are listed in Supplemental Experimental Procedures. ChIP analyses on cell lines (Min6 and α-TC1) were performed using the Millipore Chromatin Immunoprecipitation Kit (Catalog No. 17-295; Millipore) according to manufacturer's instructions, with minor modifications described before (Dhawan et al., 2009).

Statistical Methods

All data are expressed as mean ± SE. Mean and SEM values were calculated from at least triplicates of a representative experiment. The statistical significance of differences was measured by unpaired Student's t test. A p value <0.05 indicated statistical significance. *p < 0.05, **p < 0.01, ***p < 0.005.

Antibodies used for coimmunoprecipitation and ChIP, procedures for quantification of global DNA methylation, and identification of proteins by liquid chromatography, mass spectrometry, and primers used for real-time PCRs for RNA expression analysis, quantification of ChIPs, and for bisulfite-sequencing analysis are presented in Supplemental Experimental Procedures.

SUPPLEMENTAL INFORMATION

Supplemental Information includes Supplemental Experimental Procedures and six figures and can be found with this article online at doi:10.1016/j.devcel.2011.03.012.

ACKNOWLEDGMENTS

We are grateful to Shaun Fouse for help with the DNA methylation analyses, Bing Li (Kurdistani Lab) and Wei Xei (Grunstein lab) for advice on MeDIP-ChIP experiments, and Murtaza Kanji and Lendy Le for technical help. We also thank the Greenberg lab, Harvard Medical School, for the Flag-MeCP2 construct. The mass spectrometry analysis was performed in the W. M. Keck Proteomic Facility at the UCLA Molecular Instrumentation Center, which was established with a grant from the W. M. Keck Foundation. S.G. is supported by an NIDDK Career Development Award. This work was supported by grants from NIDDK (DK080996, DK068763), Beta Cell Biology Consortium (DK089532), Juvenile Diabetes Research Foundation, and the Helmsley Trust to A.B. S.D. and S.G. performed the experiments and analyses. G.F. provided the *Dnmt1*$^{lox/lox}$mice. A.B., S.D., and S.G. conceived and planned the experiments and interpreted data. S-i.T. provided technical assistance. A.B. and S.D. wrote the manuscript.

Received: December 22, 2010
Revised: February 25, 2011
Accepted: March 18, 2011
Published: April 18, 2011

REFERENCES

Bird, A. (2002). DNA methylation patterns and epigenetic memory. Genes Dev. *16*, 6–21.

Brennand, K., Huangfu, D., and Melton, D. (2007). All beta cells contribute equally to islet growth and maintenance. PLoS Biol. *5*, e163.

Collombat, P., Mansouri, A., Hecksher-Sorensen, J., Serup, P., Krull, J., Gradwohl, G., and Gruss, P. (2003). Opposing actions of Arx and Pax4 in endocrine pancreas development. Genes Dev. *17*, 2591–2603.

Collombat, P., Hecksher-Sorensen, J., Broccoli, V., Krull, J., Ponte, I., Mundiger, T., Smith, J., Gruss, P., Serup, P., and Mansouri, A. (2005). The simultaneous loss of Arx and Pax4 genes promotes a somatostatin-producing cell fate specification at the expense of the alpha- and beta-cell lineages in the mouse endocrine pancreas. Development *132*, 2969–2980.

Collombat, P., Hecksher-Sorensen, J., Krull, J., Berger, J., Riedel, D., Herrera, P.L., Serup, P., and Mansouri, A. (2007). Embryonic endocrine pancreas and mature beta cells acquire alpha and PP cell phenotypes upon Arx misexpression. J. Clin. Invest. *117*, 961–970.

Collombat, P., Xu, X., Ravassard, P., Sosa-Pineda, B., Dussaud, S., Billestrup, N., Madsen, O.D., Serup, P., Heimberg, H., and Mansouri, A. (2009). The ectopic expression of Pax4 in the mouse pancreas converts progenitor cells into alpha and subsequently beta cells. Cell *138*, 449–462.

Dahl, J.A., and Collas, P. (2008). MicroChIP—a rapid micro chromatin immunoprecipitation assay for small cell samples and biopsies. Nucleic Acids Res. *36*, e15.

Dhawan, S., Tschen, S.I., and Bhushan, A. (2009). Bmi-1 regulates the Ink4a/Arf locus to control pancreatic beta-cell proliferation. Genes Dev. *23*, 906–911.

Dor, Y., Brown, J., Martinez, O.I., and Melton, D.A. (2004). Adult pancreatic beta-cells are formed by self-duplication rather than stem-cell differentiation. Nature *429*, 41–46.

Georgia, S., and Bhushan, A. (2004). Beta cell replication is the primary mechanism for maintaining postnatal beta cell mass. J. Clin. Invest. *114*, 963–968.

Goll, M.G., and Bestor, T.H. (2005). Eukaryotic cytosine methyltransferases. Annu. Rev. Biochem. *74*, 481–514.

Guccione, E., Bassi, C., Casadio, F., Martinato, F., Cesaroni, M., Schuchlautz, H., Luscher, B., and Amati, B. (2007). Methylation of histone H3R2 by PRMT6 and H3K4 by an MLL complex are mutually exclusive. Nature *449*, 933–937.

Hanna, J., Saha, K., Pando, B., van Zon, J., Lengner, C.J., Creyghton, M.P., van Oudenaarden, A., and Jaenisch, R. (2009). Direct cell reprogramming is a stochastic process amenable to acceleration. Nature *462*, 595–601.

Herrera, P.L. (2000). Adult insulin- and glucagon-producing cells differentiate from two independent cell lineages. Development *127*, 2317–2322.

Hyllus, D., Stein, C., Schnabel, K., Schiltz, E., Imhof, A., Dou, Y., Hsieh, J., and Bauer, U.M. (2007). PRMT6-mediated methylation of R2 in histone H3 antagonizes H3 K4 trimethylation. Genes Dev. *21*, 3369–3380.

Jackson-Grusby, L., Beard, C., Possemato, R., Tudor, M., Fambrough, D., Csankovszki, G., Dausman, J., Lee, P., Wilson, C., Lander, E., et al. (2001). Loss of genomic methylation causes p53-dependent apoptosis and epigenetic deregulation. Nat. Genet. *27*, 31–39.

Jones, P.L., Veenstra, G.J., Wade, P.A., Vermaak, D., Kass, S.U., Landsberger, N., Strouboulis, J., and Wolffe, A.P. (1998). Methylated DNA and MeCP2 recruit histone deacetylase to repress transcription. Nat. Genet. *19*, 187–191.

Kirmizis, A., Santos-Rosa, H., Penkett, C.J., Singer, M.A., Vermeulen, M., Mann, M., Bahler, J., Green, R.D., and Kouzarides, T. (2007). Arginine methylation at histone H3R2 controls deposition of H3K4 trimethylation. Nature *449*, 928–932.

Klose, R.J., and Bird, A.P. (2006). Genomic DNA methylation: the mark and its mediators. Trends Biochem. Sci. *31*, 89–97.

Lee, P.P., Fitzpatrick, D.R., Beard, C., Jessup, H.K., Lehar, S., Makar, K.W., Perez-Melgosa, M., Sweetser, M.T., Schlissel, M.S., Nguyen, S., et al. (2001). A critical role for Dnmt1 and DNA methylation in T cell development, function, and survival. Immunity *15*, 763–774.

Martin, C., and Zhang, Y. (2007). Mechanisms of epigenetic inheritance. Curr. Opin. Cell Biol. *19*, 266–272.

Millar, D.S., Warnecke, P.M., Melki, J.R., and Clark, S.J. (2002). Methylation sequencing from limiting DNA: embryonic, fixed, and microdissected cells. Methods *27*, 108–113.

Miranda, T.B., and Jones, P.A. (2007). DNA methylation: the nuts and bolts of repression. J. Cell. Physiol. *213*, 384–390.

Nan, X., Ng, H.H., Johnson, C.A., Laherty, C.D., Turner, B.M., Eisenman, R.N., and Bird, A. (1998). Transcriptional repression by the methyl-CpG-binding protein MeCP2 involves a histone deacetylase complex. Nature *393*, 386–389.

Ng, R.K., Dean, W., Dawson, C., Lucifero, D., Madeja, Z., Reik, W., and Hemberger, M. (2008). Epigenetic restriction of embryonic cell lineage fate by methylation of Elf5. Nat. Cell Biol. *10*, 1280–1290.

Prado, C.L., Pugh-Bernard, A.E., Elghazi, L., Sosa-Pineda, B., and Sussel, L. (2004). Ghrelin cells replace insulin-producing beta cells in two mouse models of pancreas development. Proc. Natl. Acad. Sci. USA *101*, 2924–2929.

Rankin, M.M., and Kushner, J.A. (2009). Adaptive beta-cell proliferation is severely restricted with advanced age. Diabetes *58*, 1365–1372.

Soriano, P. (1999). Generalized lacZ expression with the ROSA26 Cre reporter strain. Nat. Genet. *21*, 70–71.

Sosa-Pineda, B., Chowdhury, K., Torres, M., Oliver, G., and Gruss, P. (1997). The Pax4 gene is essential for differentiation of insulin-producing beta cells in the mammalian pancreas. Nature *386*, 399–402.

Takahashi, K., and Yamanaka, S. (2006). Induction of pluripotent stem cells from mouse embryonic and adult fibroblast cultures by defined factors. Cell *126*, 663–676.

Takizawa, T., Nakashima, K., Namihira, M., Ochiai, W., Uemura, A., Yanagisawa, M., Fujita, N., Nakao, M., and Taga, T. (2001). DNA methylation is a critical cell-intrinsic determinant of astrocyte differentiation in the fetal brain. Dev. Cell *1*, 749–758.

Teta, M., Rankin, M.M., Long, S.Y., Stein, G.M., and Kushner, J.A. (2007). Growth and regeneration of adult beta cells does not involve specialized progenitors. Dev. Cell *12*, 817–826.

Thorel, F., Nepote, V., Avril, I., Kohno, K., Desgraz, R., Chera, S., and Herrera, P.L. (2010). Conversion of adult pancreatic alpha-cells to beta-cells after extreme beta-cell loss. Nature *464*, 1149–1154.

Tschen, S.I., Dhawan, S., Gurlo, T., and Bhushan, A. (2009). Age-dependent decline in beta-cell proliferation restricts the capacity of beta-cell regeneration in mice. Diabetes *58*, 1312–1320.

Vierbuchen, T., Ostermeier, A., Pang, Z.P., Kokubu, Y., Sudhof, T.C., and Wernig, M. (2010). Direct conversion of fibroblasts to functional neurons by defined factors. Nature *463*, 1035–1041.

Weber, M., Davies, J.J., Wittig, D., Oakeley, E.J., Haase, M., Lam, W.L., and Schubeler, D. (2005). Chromosome-wide and promoter-specific analyses identify sites of differential DNA methylation in normal and transformed human cells. Nat. Genet. *37*, 853–862.

Xie, W., Song, C., Young, N.L., Sperling, A.S., Xu, F., Sridharan, R., Conway, A.E., Garcia, B.A., Plath, K., Clark, A.T., et al. (2009). Histone h3 lysine 56 acetylation is linked to the core transcriptional network in human embryonic stem cells. Mol. Cell *33*, 417–427.

Zhong, L., Georgia, S., Tschen, S.I., Nakayama, K., and Bhushan, A. (2007). Essential role of Skp2-mediated p27 degradation in growth and adaptive expansion of pancreatic beta cells. J. Clin. Invest. *117*, 2869–2876.

Zhou, Q., Brown, J., Kanarek, A., Rajagopal, J., and Melton, D.A. (2008). In vivo reprogramming of adult pancreatic exocrine cells to beta-cells. Nature *455*, 627–632.